

RESEARCH ARTICLE

A Conserved GPG-Motif in the HIV-1 Nef Core Is Required for Principal Nef-Activities

Marta Martínez-Bonet¹, Claudia Palladino^{1,2a}, Veronica Briz^{1,2b}, Jochen M. Rudolph^{2,3c}, Oliver T. Fackler², Miguel Relloso¹, Maria Angeles Muñoz-Fernandez¹, Ricardo Madrid^{3,*}

1 Laboratorio de Inmunobiología Molecular, Instituto de Investigación Biomédica Gregorio Marañón (IISGM), 28007 Madrid, Spain, **2** Department of Infectious Diseases, Integrative Virology, University Hospital Heidelberg, Heidelberg, Germany, **3** Department of Virology, Centro de Biología Molecular Severo Ochoa, CSIC/UAM, Madrid, Spain

^{2a} Current address: Unidade dos Retrovírus e Infecções Associadas, Centro de Patogénese Molecular e Instituto de Investigação do Medicamento (iMed.Ulisboa), Fac. Farmácia, Universidade de Lisboa, Lisboa, Portugal

^{2b} Current address: Viral Infection and Immunity Unit, National Centre for Microbiology, Instituto de Salud Carlos III (ISCIII), Madrid, Spain

^{2c} Current address: Institut für Molekulare und Klinische Immunologie, Medizinische Fakultät Otto-von-Guericke-Universität Magdeburg, Magdeburg, Germany

* ricardo-m@cbm.csic.es



OPEN ACCESS

Citation: Martínez-Bonet M, Palladino C, Briz V, Rudolph JM, Fackler OT, Relloso M, et al. (2015) A Conserved GPG-Motif in the HIV-1 Nef Core Is Required for Principal Nef-Activities. PLoS ONE 10(12): e0145239. doi:10.1371/journal.pone.0145239

Editor: Yuntao Wu, George Mason University, UNITED STATES

Received: June 20, 2015

Accepted: November 30, 2015

Published: December 23, 2015

Copyright: © 2015 Martínez-Bonet et al. This is an open access article distributed under the terms of the [Creative Commons Attribution License](https://creativecommons.org/licenses/by/4.0/), which permits unrestricted use, distribution, and reproduction in any medium, provided the original author and source are credited.

Data Availability Statement: All relevant data are within the paper and its Supporting Information files.

Funding: This work was supported by the Ramon y Cajal research program (MCIIN-RYC-2005-002174; <http://www.mineco.gob.es/portal/site/mineco/idi>), Fondo de Investigación Sanitaria en España (FIS-PS09/01386; <http://www.isciii.es/>) to RM, and Comunidad de Madrid (S-2010/BMD-2332; <http://www.madridmasd.org/>) to MAM-F, and the Deutsche Forschungsgemeinschaft (TRR83, project 15 to OTF). MM-B, CP and VB hold a fellowship from the Fondo de Investigación Sanitaria en España (FIS, <http://www.isciii.es/>). The funders had no role in study

Abstract

To find out new determinants required for Nef activity we performed a functional alanine scanning analysis along a discrete but highly conserved region at the core of HIV-1 Nef. We identified the GPG-motif, located at the 121–137 region of HIV-1 NL4.3 Nef, as a novel protein signature strictly required for the p56^{Lck} dependent Nef-induced CD4-downregulation in T-cells. Since the Nef-GPG motif was dispensable for CD4-downregulation in HeLa-CD4 cells, Nef/AP-1 interaction and Nef-dependent effects on Tf-R trafficking, the observed effects on CD4 downregulation cannot be attributed to structure constraints or to alterations on general protein trafficking. Besides, we found that the GPG-motif was also required for Nef-dependent inhibition of ring actin re-organization upon TCR triggering and MHCI downregulation, suggesting that the GPG-motif could actively cooperate with the Nef PxxP motif for these HIV-1 Nef-related effects. Finally, we observed that the Nef-GPG motif was required for optimal infectivity of those viruses produced in T-cells. According to these findings, we propose the conserved GPG-motif in HIV-1 Nef as functional region required for HIV-1 infectivity and therefore with a potential interest for the interference of Nef activity during HIV-1 infection.

Introduction

Nef is a myristoylated accessory protein of about 25- to 34 kDa produced early and abundantly upon infection by HIV-1, HIV-2 or SIV. Nef is a molecular regulator of HIV-1 infectivity and pathogenesis and its expression increases virus titers by more than two logs during the early phase of infection [1,2]. This feature likely favours initial viral spread and the onset of AIDS in

design, data collection and analysis, decision to publish, or preparation of the manuscript.

Competing Interests: The authors have declared that no competing interests exist.

infected patients [3,4,5,6]. Nef is a multifunctional viral protein designed to interact with different host factors. Among the different interaction sites described so far, Nef protein includes a Proline-rich domain ($_{72}\text{PxxP}_{75}$) that allows interaction with the SH3 domain of the Src family tyrosine kinase proteins (as Hck, Lyn and lymphocyte-specific protein tyrosine kinase p56^{Lck}); the acidic motif ($_{61}\text{EEEE}_{64}$) that mediates the interaction with PACS-1 protein, and the di-Leucine domain ($_{160}\text{ExxxLL}_{165}$), involved in the interaction with the clathrin adaptor complexes AP-1, AP-2 and AP-3 [7]. Mainly through direct protein-protein interactions, the Nef's hallmark lies on its ability to fine-tune the intracellular transport and signal transduction processes to optimize viral replication and spread ([8,9] for review). Additionally, HIV-1 Nef contributes to the escape of HIV-1-infected cells from immunosurveillance by altering the subcellular localization of several key proteins in the immune response such as CD4 [10], MHCI [11], CD28 [12], CD8b [13], CXCR4 [14], CCR5 [15], MHCII [16], and DC-SIGN [17], mainly through the recruitment of the ubiquitous adaptors complexes AP-1 and AP-3 [18,19,20,21], impairing the endocytic and the anterograde trafficking routes in infected cells [22,23].

Consider the Nef-induced CD4-downregulation from the plasma membrane. Although Nef is able to inhibit its recycling and promote its recruitment into late endosomes towards protein degradation in all the cell types tested so far, HIV-1 Nef is further able to boost the internalization rate of CD4 but only in lymphoid cells [24]. This early effect has been broadly accepted to occur through the impairment of p56^{Lck} -mediated CD4-membrane stabilization by Nef [25]. Indeed, it has been demonstrated that Nef should first disrupt the p56^{Lck} /CD4 interaction to unmask the CD4 di-Leucine motif and subsequently recruits AP-2 to discrete regions of the plasma membrane to enhance CD4 internalization rates [24,25,26].

Besides its role in CD4 stabilization at plasma membrane, p56^{Lck} is also central for HIV-1 Nef activity at tuning the activation levels in infected CD4+ T cells and extending their life-span during viral replication. In particular, HIV-1 Nef affects the phosphorylation status of p56^{Lck} , its activity and induces its redistribution into an intracellular compartment (IC) located at the Recycling Endosomes/Trans-Golgi Network (RE/TGN) level [25,27,28,29]. This effect on p56^{Lck} is a well conserved feature along Nef proteins [30]. At molecular level, the integrity of the Nef-PxxP domain is required for the related effects of HIV-1 Nef on p56^{Lck} . Studies on Nef/ p56^{Lck} interaction indicate that the Nef-PxxP domain is required but not sufficient to allow the binding to p56^{Lck} , since the interaction with the p56^{Lck} -SH2 domain synergistically enhances the binding of HIV-1 Nef and p56^{Lck} [25,31]. The PxxP motif is also essential for downregulation of MHCI [32], as well as for the association of Nef with the cellular kinase PAK2, which causes the phosphorylation and thereby inactivation of the actin severing factor cofilin, inducing cytoskeletal rearrangements and thus preventing the formation of F-actin rich circumferential rings [33,34].

In this study, we identified a novel functional motif in a highly conserved loop in Nef proteins, the GPG-motif, required for the main activities of HIV-1 Nef, such as CD4-downregulation, p56^{Lck} recruitment and optimal infectivity of viruses produced in T-lymphocytes, and involved in ring actin re-organization inhibition and MHCI downregulation.

Therefore, we propose the Nef-GPG motif as target for therapeutic intervention to restrict key Nef activities during the early phases of infection and dissemination of HIV-1.

Materials and Methods

Plasmid constructs

pCG-Nef-GFP, pGEX-Nef or pCDNA-Nef-HA for the expression of Nef-GFP, GST-Nef and Nef-HA constructs, respectively, were generously donated by S. Benichou (Institut Cochin,

Paris, France) and used as templates for paired mutagenesis (Quick-change site directed mutagenesis Stratagene, La Jolla, CA) in the 123–137 region of HIV-1 Nef using specific mutagenic primers (S1 Table). Correctness of mutations was verified by automated DNA sequencing and blast analysis. X4-tropic strain pNL4.3 (HIV-1 wt) and pNL4.3 Δ nef (HIV Δ nef) (NIH; NIH AIDS Research and Reference Reagent Program, Division of AIDS, NIAID). p56^{Lck}-GFP and p56^{Lck}-mCherry constructs were obtained by the fusion of full-length human p56^{Lck} cDNA in pEGFP-N1 or pmCherry N1 (Clontech), respectively.

Antibodies

Mouse antibodies for γ -adaplin and GFP were obtained from Sigma; rat anti-HA clone 3E10 was from Roche; anti-human CD4 mAbs clone 4B12 and clone OKT4 were from Santacruz and Leica; purified anti-MCHI mAb (WG-32) was kindly donated by A. Corbí (CIB-CSIC, Madrid); anti-Tf-R mAb was from Zymed and Alexa-594 Transferrin conjugate was from Molecular Probes. Anti-p56^{Lck} mAb was from BD Transduction Laboratories and pTyr505-Lck mAb was from Millipore. PE-, PC7-conjugated anti-human CD4 mAbs, PE-conjugated anti-CD3 mAb, and PE- and PC7-conjugated anti-mouse immunoglobulin G were purchased by BD Pharmingen. Secondary antibodies Alexa-555- or Alexa-647- conjugated anti-murine, and Alexa-555-conjugated anti-rat were from Molecular Probes. For T cell spreading, the monoclonal antibody (mAb) anti-CD3 (clone HIT3a) was used (BD Pharmingen). For F-actin stain, tetramethylrhodamine isothiocyanate (TRITC)-phalloidin (Sigma) was used. For Western blotting, secondary horseradish peroxidase-conjugated anti-IgGs were from Dako.

Cells and transfections

HeLa P4R5 MAGI, HeLa TZM-bl (NIH; NIH AIDS Research and Reference Reagent Program, Division of AIDS, NIAID) and HEK 293T cells (ATCC number CRL-11268, Rockefeller University) were grown in DMEM plus glutamine, antibiotics and 5% decompartmented-FCS (foetal calf serum) (GibcoBRL, Invitrogen). HeLa P4R5 MAGI cell cultures were supplemented with 100 mg/mL geneticin and 1 mg/mL puromycin. T-cell lines were maintained in RPMI with 10% FCS and supplemental glutamine, penicillin, and streptomycin. For experiments with human primary T cells, the CD3+CD4+ T cell subpopulation was obtained by negative selection (Miltenyi) from freshly PBMC from healthy donors and immediately activated for 3 days with 1 μ g/mL PHA, 30 U/mL IL2 in RPMI with 10% fetal bovine serum and supplemented with glutamine, penicillin, and streptomycin. CEM-SS and Jurkat cells (NIH; NIH AIDS Research and Reference Reagent Program, Division of AIDS, NIAID) as well as isolated primary T-lymphocytes were transfected by electroporation using the Nucleofector I device (Lonza) according to manufacturer's guidelines. HeLa and HEK-293T cells were transfected using Lipofectin (Invitrogen).

Flow cytometry analysis of CD4 downregulation

CEM-SS cells, HeLa P4R5 MAGI or primary T-cells were transfected with 20 μ g of plasmids expressing wild-type or mutated Nef-GFP plasmids. When specified, HeLa P4R5 MAGI cells were cotransfected with 5 μ g of p56^{Lck}-GFP plasmid and 10 μ g of plasmids expressing wild type or mutated Nef-HA. After 16 h, cells were stained for 1 h at 4°C with the corresponding conjugated antibodies in FACS staining buffer (phosphate-buffered saline, PBS) with 2% fetal bovine serum and IgGs from murine serum (SIGMA). Specific staining in CEM-SS and HeLa P4R5 MAGI cells was analysed by two-colour flow cytometry, whereas in primary T-cells three-colour flow cytometry was carried out in a FACSCalibur flow cytometer (Becton

Dickinson). FlowJo software (FLOWJO LLC. <http://www.flowjo.com/>) was used to quantify the mean fluorescence intensity (MFI) of non-transfected and transfected cells. The mean fluorescence intensity (MFI) of the GFP-positive cells was used to calculate the % of activity of each mutant in reducing the surface expression of CD4 relative to wild-type Nef and expressed as the mean \pm SD of three different assays done in duplicate.

Flow cytometry analysis of MHCI downregulation

CEM-SS cells were transfected with 15 μ g of plasmids expressing wild-type or mutated Nef-GFP plasmids. After 24 h, the cells were first stained for 1h at 4°C with an anti-MHCI antibody and then stained with a secondary PE-conjugated antibody in FACS staining buffer. Specific staining was analysed by two-colour flow cytometry using a FACSCalibur flow cytometer (Becton Dickinson). FlowJo data analysis software (FLOWJO. LLC. <http://www.flowjo.com/>) was used to quantify the mean fluorescence intensity (MFI) of nontransfected and transfected cells. The MFI of the GFP-positive cells was used to calculate the % of activity of each mutant in reducing the surface expression of MCHI relative to wild-type Nef and expressed as the mean \pm SD of three different assays done in duplicate.

Indirect immunofluorescence confocal microscopic analysis

CEM-SS, Jurkat, primary T-cells or HeLa P4R5 MAGI cells spread on poly-L-lysine (Sigma) and normal glass coverslips, respectively, were stained for immunofluorescent analysis as described [22]. Cells were fixed in formalin (Sigma), quenched for 5 min with 0.1% (wt/vol) BSA in PBS, and permeabilized or not with 0.1% Triton-X100 (Sigma) in PBS at 4°C for 5 min, rinsed, incubated with 1% (wt/vol) BSA (Sigma) for 30 min. Cells were then incubated successively with the primary and the appropriate fluorescent secondary antibody for 1h at room temperature. For double-labelling experiments, a sequential immunostaining procedure was followed. Cell surface staining of markers was carried out at 4°C in non permeabilized cells prior to fixation. Suitable controls to assess the specificity of the labelling were performed. After thorough washing, coverslips were mounted on slides using Fluoromount-G (Southern-Biotech). Images were acquired using a confocal laser microscope (Leica TCS SP5, Leica Microsystems). Fluorescence acquisition was performed using the 488-, 561- or 647-nm laser lines. For deconvolution Huygens 3.0 software was used and images were processed using Adobe Photoshop software. For each sample, three medial optical 0.5 μ m slices of 50 different cells were recorded. Image J software (National Institutes of Health; (<http://rsb.info.nih.gov/ij/index.html>)) was used to quantify the intensity of fluorescence (mean intensity of fluorescence per pixel) of CD4, p56^{Lck}, pY505-Lck, Tf-R distribution at the plasma membrane or endosomal compartments in the three medial confocal sections using a 0–250 gray color scale. For the quantitative analysis of p56^{Lck} distribution in Jurkat and PBLs, the p56^{Lck} fluorescence signal plotted along 8 radial lines at the equatorial plane of the cell using the Image J and the delimited surfaces were measured. The ratio of internal to plasma membrane fluorescence of p56^{Lck} was calculated for each mutant in three independent experiments (n = 25 cells). Cells with a ratio greater than or equal to the mean number of non-transfected cells+2 \times SEM were considered to express high levels of p56^{Lck} at intracellular compartments. Only 8% of non-transfected cells met this standard. The confidence limits of the results were assessed by Student's *t* test.

Transferrin uptake assays

16h after transfection, CEM cells were attached to poly-L-lysine glass coverslips and starved in serum-free medium (containing 0.1% BSA, 10 mM HEPES) for 2 h at 37°C. Cells were then incubated at 37°C for 20 min in the same medium containing 10 μ g/ml Tfn-Alexa-594. Cells

were washed, fixed, and then analysed by confocal microscopy (Leica TCS SP5, Leica Microsystems). Double fluorescence acquisition was performed using the 488- and 561-nm laser lines. In each experiment, the laser beam and the photomultipliers were adjusted to the Alexa signal of non-transfected cells. For each sample, three medial optical 0.5 μm slices of 50 different cells were recorded. NIH Image software was used to quantify the intensity of fluorescence (mean intensity of fluorescence per pixel) of Tfn-594 staining on the whole cells using a 0–250 grayscale. The confidence limits of the results were assessed by Student's *t* test. For deconvolution we used Huygens 3.0 software was used and images were processed using Adobe Photoshop software.

Analysis of TCR-mediated actin ring formation

T-cell spreading on stimulatory surfaces was performed essentially as described [35]. Briefly, microscope cover glasses were coated with anti-CD3 antibody diluted in TBS (10 $\mu\text{g}/\text{ml}$) for 3h at 37°C. After washing with TBS, the cover glasses were stored in TBS at 4°C. Cells were added in a volume of 50 μl onto the glasses, incubated for 5 min at 37°C and fixed by direct addition of 4% PFA. Cell were then permeabilized as described above and incubated with TRITC-phalloidin for 5 min at RT. Further steps were performed as described above.

GST pull-down assay

Full length Nef protein fused to glutathione-S-transferase (GST) was produced in DH5 α *E.coli* cells and purified by affinity using GSH-Sepharose beads (Amersham Biosciences). For Nef/AP-1 binding, HeLa cells ($5 \cdot 10^6$) were lysed in Lysis buffer (25 mM Tris-HCl pH 7.4, 2 mM EDTA, 120 mM NaCl, 1% glycerol, 0,5% Triton and protease inhibitors). The cleared lysates were incubated for 2h or overnight at 4°C with 3 μg of GST or GST-Nef proteins immobilized on glutathione (GSH)-Sepharose beads. Then, beads were washed three times in lysis buffer, and the bound cellular proteins were analysed by Western blotting using the appropriate antibodies. The chemiluminescent signals were quantified using Image J.

Viral infectivity

Virions were transduced by transient transfection of Jurkat ($6 \cdot 10^6$) or HEK 293T cells ($5 \cdot 10^6$) with 20 μg of proviral pNL43-wt, or 20 μg of proviral pNL43- Δnef plasmid along 60 μg of empty PCI or expression plasmids for wild-type or mutated Nef-HA. 72h post-transfection, virion-containing culture supernatants were harvested, pre-cleared by centrifugation at 1,200 rpm for 7 min and filtered through a 0.45- μm -pore-size membrane. The concentration of p24 antigen in viral stocks was measured by a quantitative enzyme-linked immunosorbent assay, ELISA (Immunogenetics), prior infectivity assays in TZM-bl cells. TZM-bl cells were infected as already described [36]. Briefly, cells were seeded one day before, infected with 20 ng p24/ 10^6 cells, and incubated for 3h at 37°C. Then, cells were incubated to 37°C upon removal of unbound virus by extensive washes. 48h after infection, TZM-bl cells were lysed using Glo-Lysis buffer (Promega) and luciferase assays were performed according to manufacture recommendations (Promega). Luminescence was measured in a VICTOR luminometer. Results were normalized to a value of 100% infectivity and represented as mean \pm SEM of relative luciferase units.

Analysis of 3D structure

Structural 3D models were built using Pymol software (Schrödinger, LLC) from the PDB file DOI:10.2210/pdb2nef/pdb at <http://www.rcsb.org/pdb/home/home.do>

Western blot analysis

Expression of wild-type and mutated Nef-GFP, p56^{Lck}-GFP, Nef-HA, endogenous p56^{Lck}, p56^{Lck}-Cherry, or γ -adaptin, from transfected cells was analysed by Western blotting using anti-GFP, HA, anti-p56^{Lck} and anti- γ -adaptin primary antibodies. Image J was used to quantify the blots.

Ethics statement

Freshly isolated T lymphocytes from healthy donors were used following the guidelines of the Bioethics Committee of the Spanish Research Council and the institutional management committee of the Centro de Biología Molecular “Severo Ochoa”. Human peripheral blood mononuclear cells (PBMC) were isolated from buffy coats of healthy informed subjects provided by the Madrid Transfusion Centre (http://www.madrid.org/cs/Satellite?language=es&pagename=CentrodeTransfusion%2FPage%2FHLLAV_home) following national guidelines.

Statistics

p values indicate statistical significance as determined by Student's t test (*, $p < 0.05$; **, $p < 0.01$; ***, $p < 0.001$).

Results

Identification of the GPG-motif in HIV-1 Nef

We piled-up the HIV-1, HIV-2 and SIV Nef protein sequences available at the Los Alamos HIV database (consulted in January 2015) to unveil new determinants involved in HIV-1 Nef's effects, using the Clustal Omega software (<http://www.ebi.ac.uk/Tools/msa/clustalo/>). Among the overall similarities found we focused on the conserved region 125 to 136 of HIV-1 NL4.3 Nef, represented by the consensus sequence QNYTXGPGØRYYP (Fig 1A and 1B).

This uncharacterized region forms a small loop between the two anti-parallel β -strands (β 2: NYT and β 3: VRYP) that expose the hydrophobic PGPG residues at the surface of Nef (Fig 1C). Consequently and because of its conservation along the different Nef alleles, we will hereafter refer to this region as the GPG-loop. This loop is located immediately downstream of the dimerization (₁₂₁FPD₁₂₃), not close to the SH3-binding Proline-rich (₆₉PxxP₇₅) or to the di-Leucine motif (₁₆₀ENTSL₁₆₅).

Mutations on the Nef-GPG loop abrogate Nef-induced CD4 downregulation in T-cells

We first explored the potential requisite of the GPG-loop for HIV-1 Nef's effects on CD4 downregulation. CEM T-cells were transfected with expression constructs coding the different Nef-GPG mutants (Table 1) and screened for CD4 surface expression levels.

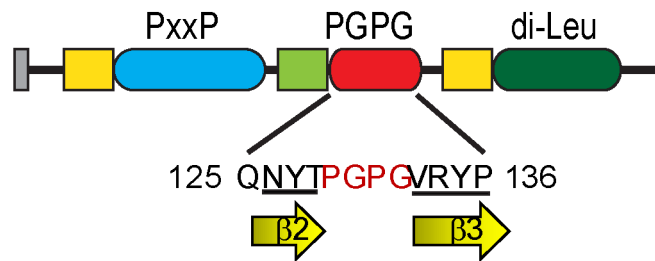
Flow cytometry analysis showed that Nef WT induced a robust reduction of CD4 cell surface levels (Fig 2A and 2B). In contrast, the YT/AA, PG2/AA, VR/AA or YP/AA mutations in the GPG-loop induced a 5–6 fold reduction in Nef-mediated CD4-downregulation, displaying surface CD4 levels close to cells expressing either the Nef-LL/AA deficient mutant (Fig 2A and 2B) or the dimerization mutants (S1A and S1B Fig).

CD4 downregulation by the Nef-QN/AA or -PG1/AA mutants was also significantly impaired but just showed a 2-fold reduction compared to wild type Nef. The reported effects of GPG mutants were not related to differences on Nef expression levels (Fig 2C), and were further confirmed in CD3+CD4+ T-cells (S1C and S1D Fig).

A

HIV-1 NL43	121 FPDWQNYTPGPGVRYPL 137
Consensus/BI.....
Consensus/C
Consensus/DI.....
Consensus/F1I.....
HIV2	I.....S.....M
HIV2UC2	I.....H.....M
SIVmac	I....D..S...I...K
ConsensusSeq.	ØPDWQNYTXGPGØRYPX

B



C

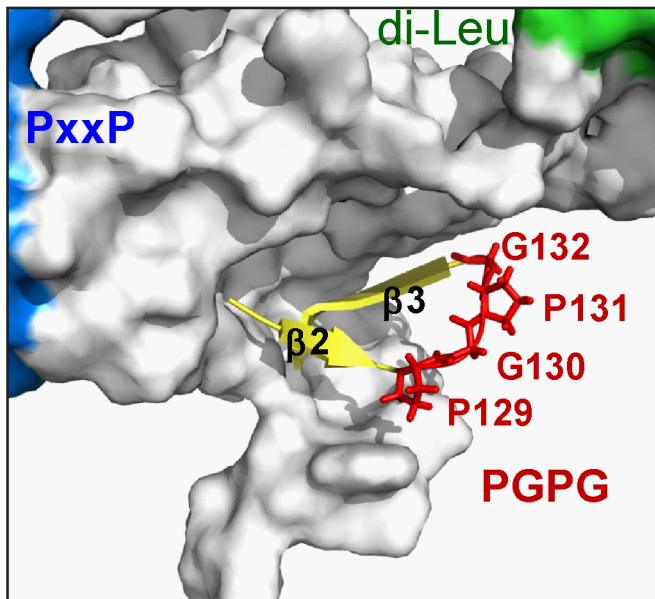


Fig 1. The GPG-loop is conserved among Nef proteins. A) Clustal W alignment of the 121–137 region of HIV-1 Nef with homologous HIV2- and SIV-Nef sequences from Los Alamos database. The consensus sequence of the GPG-loop is highlighted to indicate the amino acid identity. X represents any amino acid residue and Ø represents a hydrophobic residue. B) Schematic representation of the domain organization of HIV-1NL4.3 Nef. The novel GPG-loop (red), conserved PxxP domain (blue), the di-Leucine based motif (dark green) as well as the membrane anchorage domain (grey), the acidic clusters (orange) and the dimerization domain (light green) are shown. C) Ribbon/surface diagram showing the HIV-1 Nef-GPG loop as generated by using the Pymol software (pdb2nef). The central GPG residues (red) are flanked by hydrophobic $\beta 2$ and $\beta 3$ sheets (yellow) in HIV-1 Nef structure. PxxP and di-Leucine motifs surfaces are coloured in blue or green, respectively.

doi:10.1371/journal.pone.0145239.g001

Table 1. Amino acid sequences of wild-type and mutated HIV-1 Nef NL4.3 from Phe121 to Phe137.

HIV-1 Nef	121	FPDWQNYTPGPGVRYPL	137
D123A		-A-----	
DW/AA		-AA-----	
QN/AA		---AA-----	
YT/AA		-----AA-----	
PG1/AA		-----AA-----	
PG2/AA		-----AA-----	
VR/AA		-----AA-	
YP/AA		-----AA-	

doi:10.1371/journal.pone.0145239.t001

GPG-dependent CD4 downregulation by HIV-1 Nef is strictly related to p56^{Lck} expression

We next analysed the effects of GPG mutations on Nef-induced CD4-downregulation in p56^{Lck}-negative cells. HeLa-CD4 cells were co-transfected with the mutated Nef-GPG expression plasmids along empty or p56^{Lck} expressing vectors. Surface and total expression of CD4 was analysed by FACS (Fig 3) or immunofluorescence (S2 Fig), respectively.

Both approaches showed that the central residues of the GPG-loop were dispensable for Nef activity on CD4-downregulation in HeLa-CD4 cells. Nef WT induced a robust reduction of CD4 cell surface levels, and this effect was not significantly affected by the expression of either Nef-PG1/AA, -PG2/AA (Fig 3A), or -QN/AA (S2 Fig) compared to wild type Nef. In contrast, the Nef-YT/AA, -VR/AA and -YP/AA mutants (S2A Fig) were as defective as in T-cells. Of note, in HeLa-CD4/p56^{Lck} cells, the central Nef-GPG mutants recovered its defective phenotype since CD4-downregulation was as impaired as in T-cells (Fig 3B and S2B Fig). The reported effects of GPG mutants were not related to differences on Nef expression levels (S2C and S2D Fig).

Since the central GPG residues were required in cells expressing p56^{Lck} but dispensable for CD4-downregulation in HeLa-CD4 cells, these results indicate that their mutation does not seem to impair Nef function through structural modifications. Moreover, our data point out that the GPG-motif is a functional signature in HIV-1 Nef.

Nef-GPG motif is not involved in Nef-induced effects in endosomal trafficking

Besides CD4, HIV-1 Nef causes a general effect on membrane trafficking within the endocytic pathway in host cells that affects the expression of transferrin receptor (Tf-R) at plasma membrane [22,23,24]. Indeed, HIV-1 Nef slows down the recycling rate of Tf-R and promotes its intracellular retention without affecting its Transferrin (Tfn)-dependent internalization rate [22]. This effect has been demonstrated to be dependent on the integrity of Nef di-Leucine motif through a direct binding to and the recruitment of AP-1 and AP-3 complexes at the early/recycling endosomal compartment level [20,22].

Thus to further exclude a negative effect on key motifs required for CD4-downregulation, we analysed whether the mutations on the GPG-motif affected either the interaction of Nef with the AP-1 clathrin complex and/or the Nef-induced impairment of endosomal traffic of Tf-R.

The Nef-PG1 and -PG2 mutants did not seem to negatively affect the Nef/AP-1 interaction (Fig 4A and 4B), the Nef-induced Tf-R downregulation from cell surface (Fig 4C and 4E), or its intracellular recruitment (Fig 4D and 4F) compared to wild type Nef.

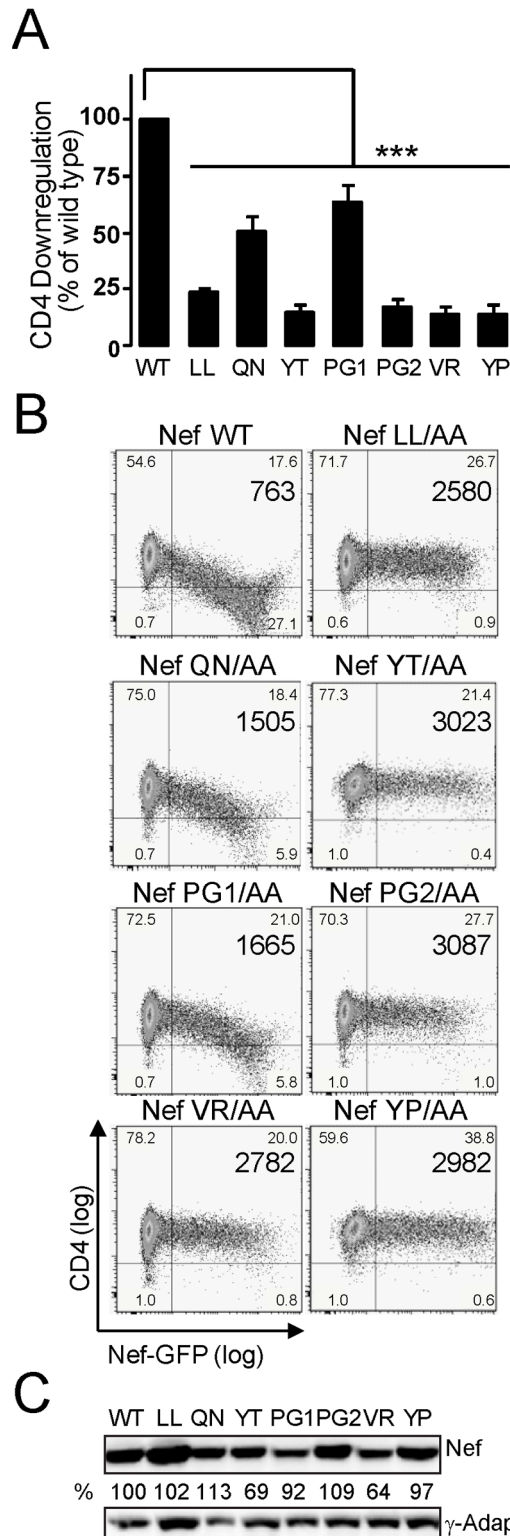


Fig 2. Mutations on the GPG-loop abrogate HIV-1 Nef-induced CD4 down-regulation. A-B) CEM cells were transfected with either wild type or the indicated Nef mutants as GFP-fusion proteins. Nef-induced surface CD4 down-regulation was analysed by two-colour flow cytometry in Nef-GFP expressing cells. The mean CD4 (PE) fluorescence intensity (MFI) of the GFP-positive cells was used to calculate the Nef activity on surface CD4 expression (A). Histograms represent the percentage of activity relative to wild-type Nef as

the arithmetic mean \pm SD of at least three independent experiments. Dot plots and the corresponding MFI are representative of three independent assays (B). ***, $p < 0.001$. C) The expression of wild type and the indicated Nef-GPG mutants in CEM cells was analysed by western blotting using an anti-GFP antibody. γ -adaplin levels were used as loading control staining.

doi:10.1371/journal.pone.0145239.g002

Therefore, our results indicate that the observed GPG-dependent effects on CD4-downregulation are not related to the integrity of the Nef di-Leucine motif. Altogether, our results suggest that the central GPG residues in Nef are not a structural but a functional motif that operates independently of the Nef di-Leucine motif to enable CD4 downregulation.

Role of the GPG-motif in Nef-dependent intracellular recruitment of pTyr-Lck

Nef expression in T-cells promotes the retargeting of p56^{Lck} from the plasma membrane to an intracellular Tf-R-positive endosomal compartment in a PxxP-dependent manner [27,28]. To validate the contribution of the GPG-motif to this Nef activity, Jurkat T-cells were transiently transfected with expression constructs for Nef-PG1/AA or -PG2/AA mutants as GFP-fusions, fixed and immuno-stained with anti-p56^{Lck} antibodies. Immunofluorescent analysis showed that Nef WT and the LL/AA mutant triggered the retargeting of p56^{Lck} from plasma membrane to an intracellular compartment. Staining with an anti-pTyr⁵⁰⁵-Lck antibody that recognizes the dually phosphorylated active pY⁵⁰⁵⁻³⁹⁴ form [29,37] indicated that the majority of this accumulated kinase was in its dually phosphorylated active form (Fig 5A and 5B).

The PG2/AA mutation significantly impaired the ability of Nef to trigger IC accumulation of p56^{Lck} (Fig 5A, right panels, and Fig 5B for quantitation), whereas the PG1/AA mutation did not have any significant effect. The reported effects of GPG mutants were not related to differences on Nef or p56^{Lck} expression levels (Fig 5C). These results were confirmed in peripheral CD3+CD4+ T-cells (S3 Fig).

Thus, the Nef-GPG motif is required for Nef-induced IC recruitment of phosphorylated p56^{Lck}.

Role of the GPG-motif in Nef's effects on TCR-induced actin remodelling and surface expression of MHC I

We also investigated the role of the Nef-GPG motif in other Nef-dependent effects. First, we analysed the Nef's effect on TCR-induced actin remodelling by tracking the formation of circumferential F-actin rich rings after TCR stimulation [38,39,40,41]. TCR engagement triggers rapid remodelling of F-actin at the plasma membrane to facilitate and sustain signal initiation and transmission. When TCR stimulation is provided by stimulatory antibodies coated to a substratum, T-cells adhere, spread and reorganize F-actin into a prominent ring structure at the cell periphery (circumferential F-actin rings). We previously established that Nef does not affect T-cell adhesion to such stimulatory surfaces but impairs their ability to subsequently spread and form circumferential F-actin rings [38,39,40,41]. This effect is strictly dependent on the interaction surface of Nef with the host cell kinase PAK2 and involves phosphorylation events mediated by Nef-associated PAK2 but also the activity of the exocyst complex that is recruited into the Nef complex by PAK2 [42]. Since Nef-PAK2 association strictly depends on the PxxP motif in Nef [43,44,45] we tested whether the GPG-motif is also required for disruption of TCR-induced actin remodelling by Nef.

Expectedly, GFP expressing control Jurkat T-cells rapidly spread on surfaces coated with anti-CD3 antibodies and formed circumferential F-actin ring in a manner undistinguishable from non-transfected neighbouring cells (see GFP expressing control cells in Fig 6A). As

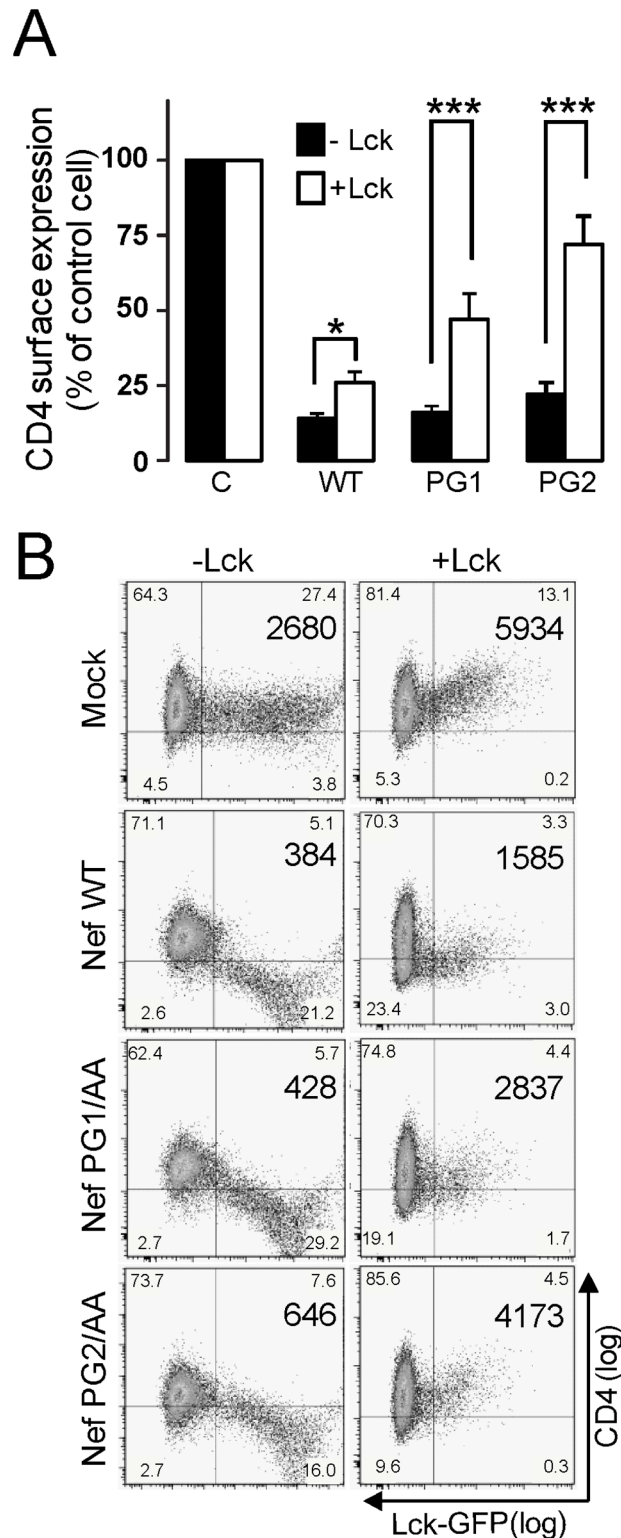


Fig 3. The integrity of the GPG-motif is dispensable for Nef-induced CD4-downregulation in p56^{Lck}-negative cells. A) HeLa-CD4 cells were co-transfected with the wild type or the indicated Nef-GPG mutants (Nef-HA) along with empty or p56^{Lck}-GFP constructs. Nef activity on CD4-downregulation was analysed by two-colour flow cytometry in GFP cells. A) Histograms represent the percentage of CD4 expression at cell surface relative to non-transfected cells. n.s., not statistically significant. ***, p < 0.001. B) Dot plots and the corresponding MFI are representative of three independent assays.

doi:10.1371/journal.pone.0145239.g003

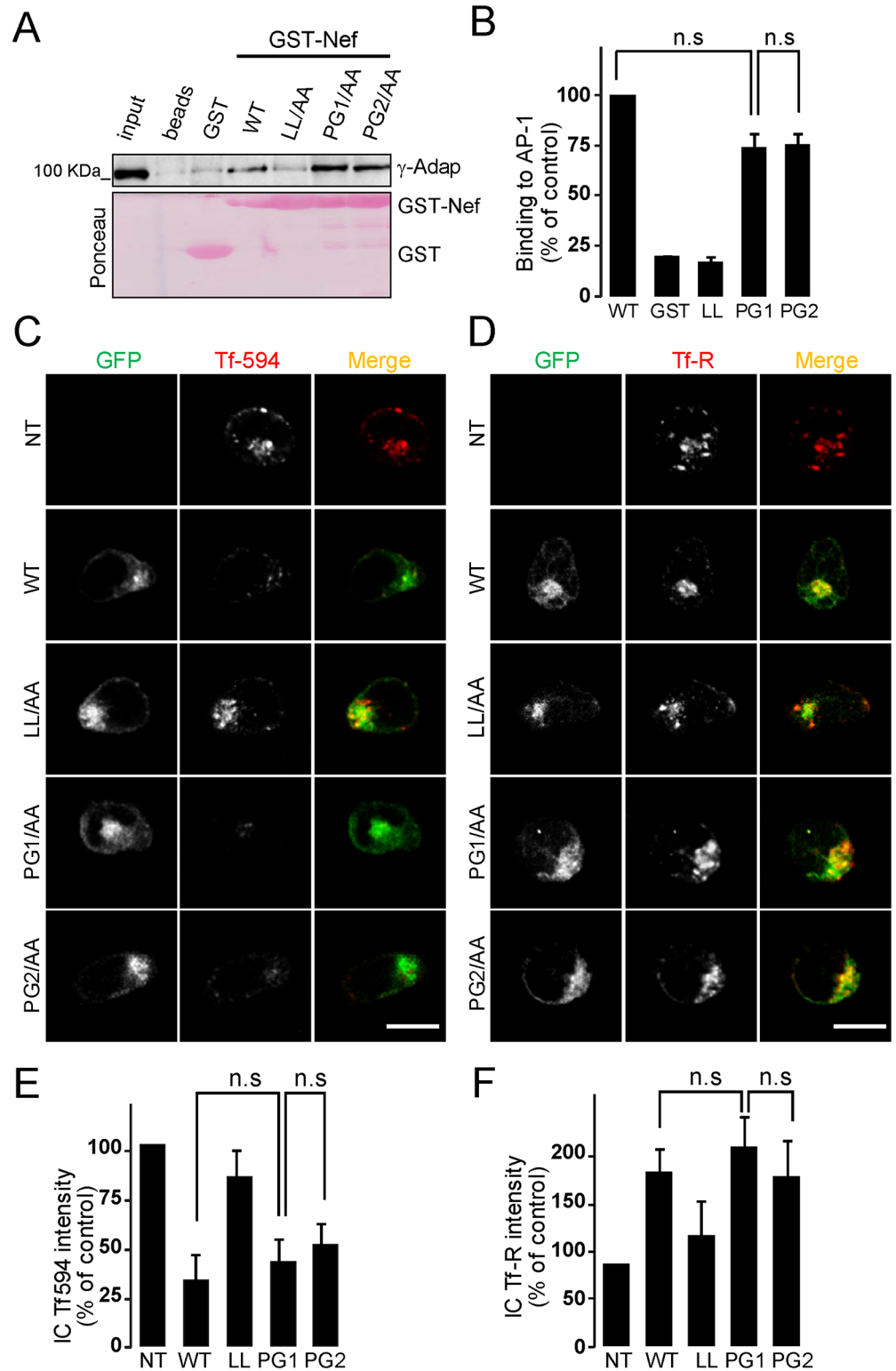


Fig 4. GPG mutations do not affect Nef-induced alteration of Tf-R trafficking. (A-B) Analysis of Nef/AP-1 interaction by *in vitro* pull-down. HeLa cell lysates were incubated with equal amounts of GSH-sepharose beads, or purified GST, wild type or the indicated Nef mutants as GST-fusions previously immobilized on GSH-sepharose beads. Bound proteins were resolved by SDS-PAGE and the association of AP-1 complex was analysed by Western blotting with anti-γ-adaptin (A) and quantified by densitometry (B). Ponceau-red

staining shows the loading of the assayed Nef-GST fusion proteins on the beads. n.s. not statistically significant. (C-D) Non-transfected, NT, or transfected CEM-T cells with expression plasmids for wild type or the indicated Nef-GPG mutants as GFP-fusion proteins were serum-starved and then incubated with Tfn-Alexa-594 for 15 min at 37°C before fixation (C), or analysed by indirect immunofluorescent staining for total Tf-R in permeabilized cells (D). Staining was visualized by confocal microscopy. A medial optical section of a representative cell is shown. Merged images show both GFP and Tfn-Alexa-594 or Tf-R labelling. Scale bar, 10 μ m. (E-F) The intensity of the fluorescence corresponding to Tfn-594 (E) or Tf-R (F) was quantified by densitometry as described under Materials and Methods. Histograms represent the percentages of the mean fluorescence intensity relative to non-transfected cells (lower panel). Values are the arithmetic mean \pm SD of at least three independent experiments in which over 50 cells were counted per condition. n.s. not statistically significant.

doi:10.1371/journal.pone.0145239.g004

established previously [30,34,38], Nef potently disrupts cell spreading and formation of F-actin rings, resulting in small rounded cells that remain attached to the surface without undergoing notable actin rearrangements (Fig 6A, note that the Nef.GFP expressing cell is less spread than non-transfected neighbouring cells and does not display prominent F-actin structures at the cell periphery). On unstimulatory surfaces T-cells adhere but do not spread or form circumferential F-actin rings and Nef-expressing cells are undistinguishable from control cells (data not shown and [46]). Upon TCR stimulation, the PG2/AA and PG1/AA mutations significantly reduced the Nef-mediated inhibition of actin dynamics and cell spreading, with effects of the PG2/AA mutation being significantly more pronounced than those of the PG1/AA mutation (Fig 6A). Quantification of over 100 cells each from three independent experiments in which cells were grouped according to their ability to spread and form circumferential F-actin rings (e.g. as the GFP expressing cells in panel A) revealed that the PG1 and PG2 mutants displayed statistically significantly less disruption of F-actin ring formation than wild type Nef but still retain residual activity (Fig 6B).

Second, we investigated the effect of the GPG-motif on Nef-induced downregulation of MHCI. In contrast to CD4, MHCI downregulation by HIV-1 Nef is not related to its interaction with p56^{Lck}, but depends on the PxxP motif [11,32,47,48]. Our results show that Nef activity on MHCI downregulation was reduced by 40% and 60% in PG1/AA or PG2/AA-expressing T-cells respectively (Fig 6C and 6D).

Together these results could indicate a weak participation of the GPG-motif in the inhibition of host cell actin dynamics and in MHCI-downregulation by HIV-1 Nef.

The Nef-GPG motif is required for Nef-dependent optimal infectivity in T-cells

Finally, we investigated the contribution of the Nef-GPG motif in Nef-dependent enhancement of viral infectivity. For this purpose wild type, Δ Nef, and Nef- PG1/AA or -PG2/AA viruses were produced in Jurkat or 293T cells, and assayed for infectivity at 48h post infection in reporter TZM-bl cells. We found that PG1/AA and PG2/AA viruses produced in Jurkat cells were as deficient as Δ Nef viruses, showing similar infectivity levels (Fig 7A).

In contrast, infectivity of viruses produced in 293T cells circumvented the requirement of integral Nef GPG-motif. Indeed, mutant PG1 and PG2 viruses produced in these cells were almost as infectious as wild type viruses (Fig 7B and Table 2). These data indicate that the GPG-motif is a new molecular determinant for Nef-dependent optimal infectivity of viruses produced in CD4+ T-cells.

Discussion

We report the identification of the HIV-Nef GPG-motif as a novel molecular determinant that contributes to Nef-induced CD4 downregulation, intracellular accumulation of

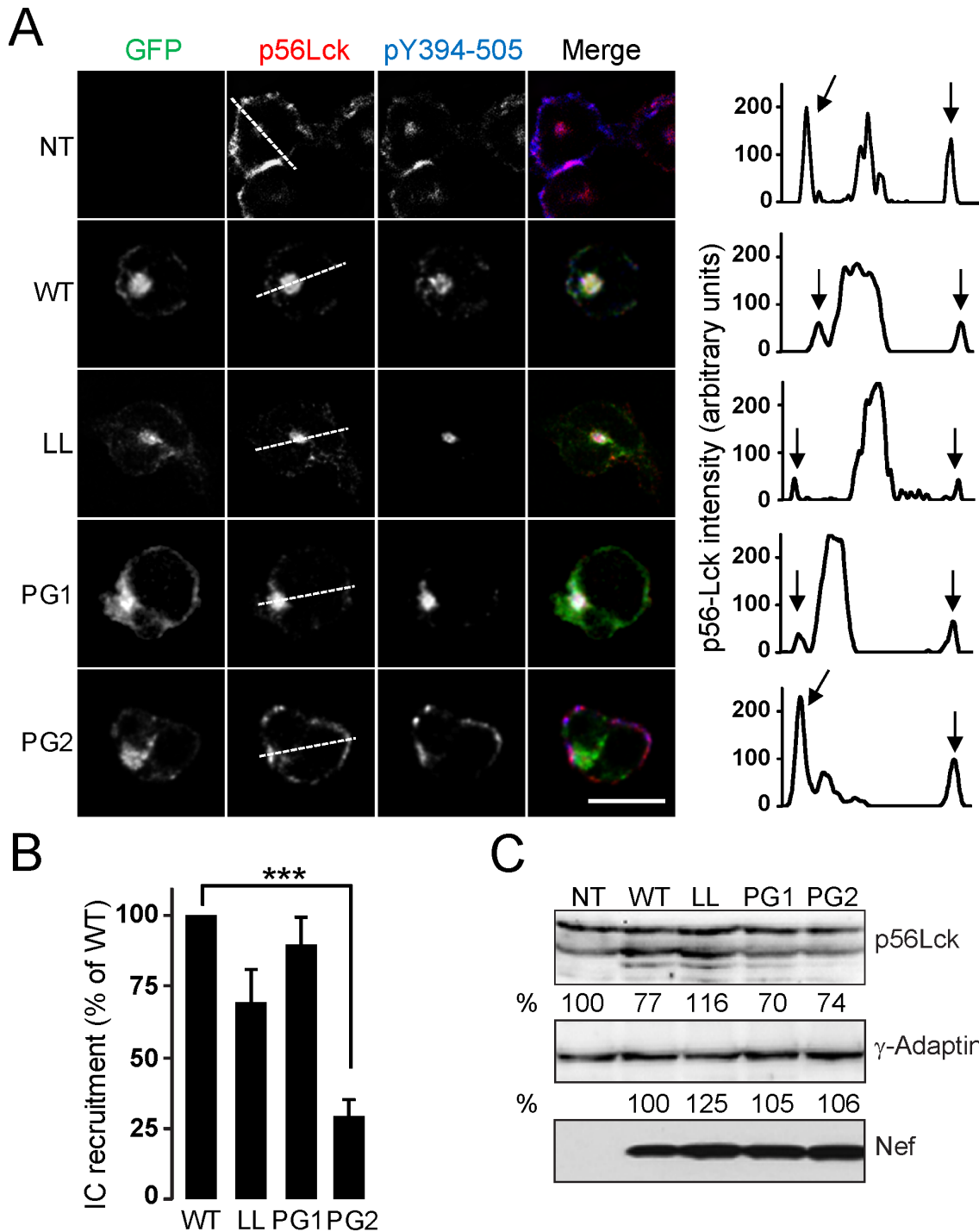


Fig 5. The GPG-motif is required for Nef-induced intracellular recruitment of p56^{Lck}. (A-B) The subcellular distribution of endogenous p56^{Lck} and pTyr-Lck was analysed by indirect immunofluorescent staining of non-transfected, NT, or transfected Jurkat cells with the expression plasmids for wild type or the indicated Nef-GPG mutants as GFP-fusion proteins. A) A medial optical section of a representative cell is shown. Densitometry analysis of the distribution of endogenous p56^{Lck} staining along the line in Jurkat cells expressing the indicated Nef-GFP proteins. Arrows indicate the position of the cell periphery (right panels). Scale bar, 10 μ m. B) Quantification of the experiment shown in A. The percentage of cells with high levels of intracellular p56^{Lck} was measured as described in Materials and Methods. Histograms represent the cells with predominant intracellular localization of p56^{Lck} compared to control cells, respectively. Values are the arithmetic mean \pm SD of at least three independent experiments in which over 100 cells were counted per condition. ***, p < 0.001. C) The expression of endogenous p56^{Lck} and transfected Nef-GFP proteins in Jurkat cells was analysed by western blotting using an anti-p56^{Lck} antibody and an anti-GFP antibody, respectively. γ -adapatin was used as loading control.

doi:10.1371/journal.pone.0145239.g005

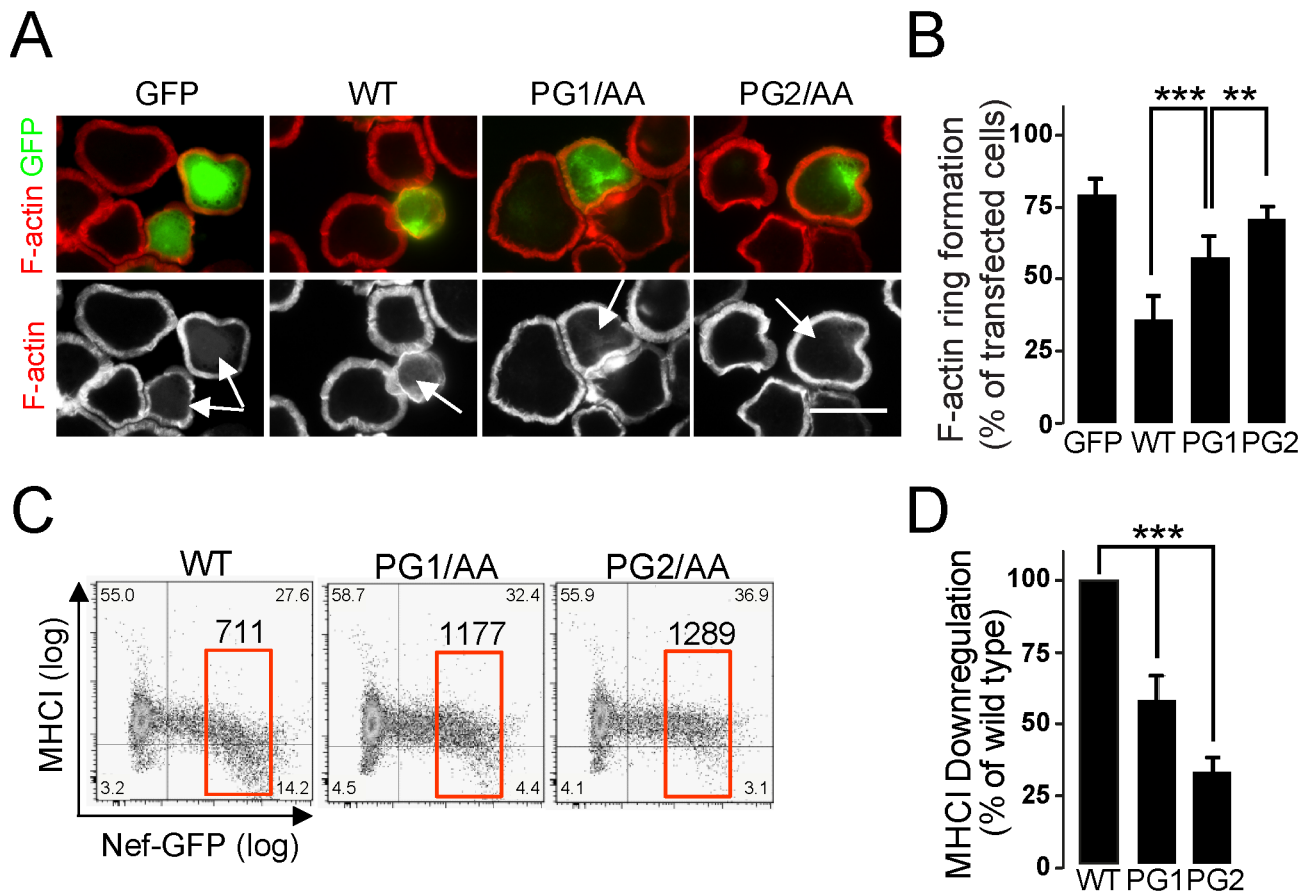


Fig 6. GPG-mutations reduce Nef-dependent inhibition of TCR-induced actin remodelling and Nef-induced down-regulation of MHC I. (A-B) Fluorescent microscopy of Jurkat T-cells transfected with the indicated GFP or Nef-GFP expression plasmids after 5 min incubation on anti-CD3 coated cover glasses and subsequent staining for F-actin. A) Depicted pictures are a representative image at the cell-cover glass level. The upper panel presents a merge of the GFP and F-actin channels, the lower panel shows the F-actin channel only. Arrows indicate transfected cells. Scale bar, 10 μ m. B) Quantification of the experiment shown in A. Shown is the percentage of cells exhibiting pronounced F-actin ring formation. Values are the arithmetic mean \pm SD of at least three independent experiments in which over 100 cells were counted per condition. ***, $p < 0.001$. (C-D) CEM cells were transfected with the wild type or the indicated Nef-GPG mutants as GFP-fusion proteins. Nef-induced surface MHC I down-regulation was assessed by flow cytometry in Nef-GFP expressing cells. C) Dot plots and the corresponding MFI are representative of three independent assays. D) The mean fluorescence intensity (MFI) of MHC I (Alexa-555) in the GFP-positive cells was used to calculate activity relative to wild-type Nef. Values are the arithmetic mean \pm SD of at least three independent experiments. **, $p < 0.01$; ***, $p < 0.001$.

doi:10.1371/journal.pone.0145239.g006

phosphorylated $p56^{\text{Lck}}$, and participates in actin-rearrangements upon TCR triggering and in MHC I downregulation. Besides and more importantly, the Nef GPG-motif was also required for Nef-enhanced HIV-1 infectivity of viruses produced in T-cells (for summary, see [Table 2](#)). Despite such a general effect on well-known Nef activities, the observed effects by the Nef-PG1 or -PG2 mutations are unlikely to rely on a potential alteration of Nef structure. This assumption is supported by the differential requirement of the Nef-GPG motif on Nef-induced CD4-downregulation in HeLa-CD4 and HeLa-CD4/ $p56^{\text{Lck}}$ cells. Moreover, our results on Nef/AP-1 interaction and Tf-R trafficking assays, strongly suggest that mutations on the GPG-motif do not promote any significant impact on those motifs required for Nef-induced impairment of endosomal trafficking. Compared to the Nef-D123A mutant, our results may also exclude any negative effect of GPG mutations on the dimerization of HIV-1 Nef. Furthermore, in agreement to a structural report on Nef [49], while the YT, VR and YP residues in the GPG-loop participate in the formation hydrogen bonds to stabilise the core $\beta 2$, $\beta 3$ and $\beta 4$

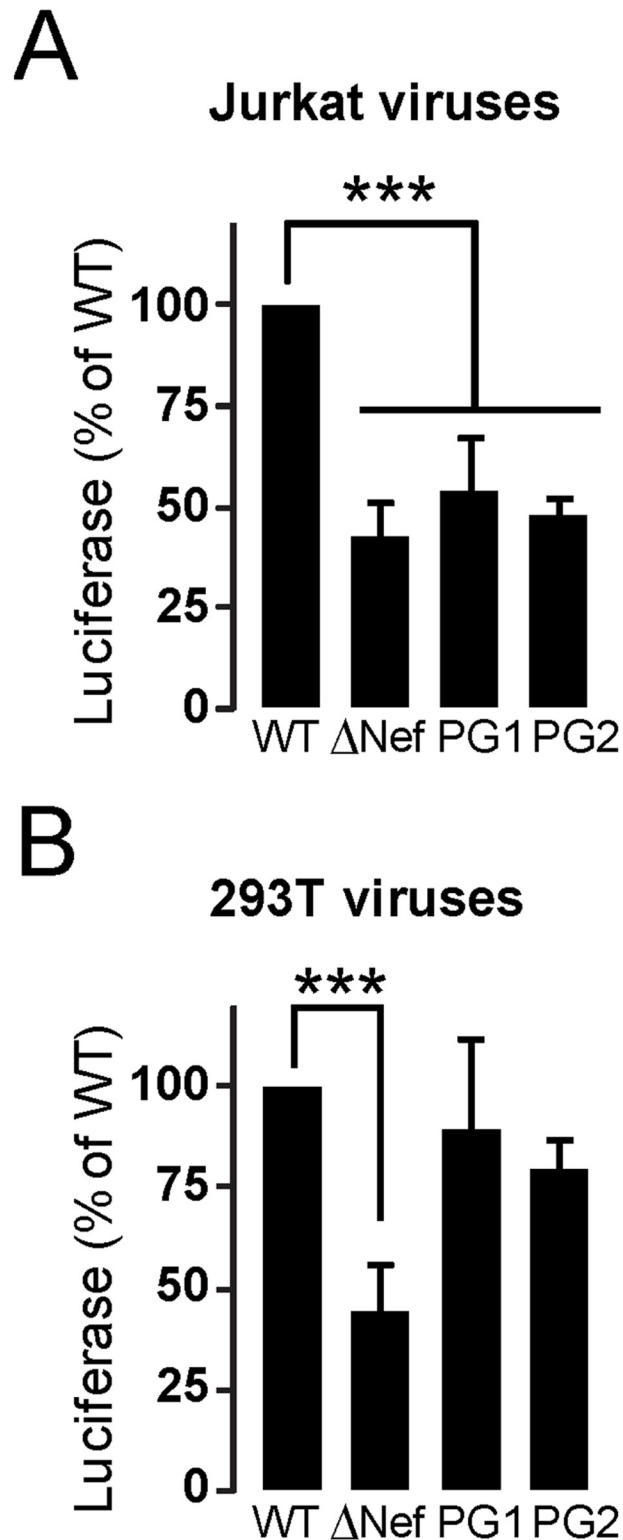


Fig 7. Nef-GPG motif is required for Nef-enhanced infectivity of HIV-1. Relative infectivity of HIV-1-expressing Nef-GPG mutations produced in Jurkat (A) or 293T (B) cells. Infectivity was analysed 48h post-infection by Luciferase assays in TZM-bl reporter cells. Results are expressed as the percentage of infectivity relative to that of the wild type viruses normalized to 100%. Values are the mean \pm SD of three independent infections, each measured in duplicate. ***, $p < 0.001$.

doi:10.1371/journal.pone.0145239.g007

Table 2. Summary of Nef-activities related to GPG-domain.

	CD4		Tf-R	AP-1	p56 ^{Lck} I.C.R	Actin ring	MHCI	Enhanced Viral Infectivity	
	+ Lck	-Lck						Jurkat	293T
WT	++	++	++	++	++	++	+	++	++
QN/AA	+	++	++*	n.d	n.d	+	-*	n.d	n.d
YT/AA	-	-	-*	n.d	n.d	-*	-*	n.d	n.d
PG1/AA	+	++	++	++	++	+	-	-	++
PG2/AA	-	++	++	++	-	-	-	-	++
VR/AA	-	-	-*	n.d	n.d	-*	-*	-*	-*
YP/AA	-	-	-*	n.d	n.d	-*	-*	n.d	n.d
DW/AA	-	-	-*	+	n.d	++*	-*	n.d	n.d
LL/AA	-	-	-	-	+	++*	+	n.d	n.d

Results are presented from this report unless otherwise indicated. CD4, CD4 downregulation; Tf-R, Tf-R downregulation and uptake of Tfn ligand; AP-1, *in vitro* binding to AP-1 complex by pull down assays; p56^{Lck} ICR, Nef-induced IC recruitment of phosphorylated p56^{Lck} Actin ring, reorganization of actin ring upon CD3-stimulation in T-cells; MHCI, MHCI downregulation; Enhancement of viral infectivity, infectivity of viruses produced by proviral transduction in either Jurkat or HEK293T cells. “++” activity of mutated Nef is >75% of wild type protein; “+” activity is between 25% and 75% of wild type; “-” activity is less than 25% of wild type; n.d. no data.

* not shown.

doi:10.1371/journal.pone.0145239.t002

sheets, the central GPG-motif conforms an hydrophobic domain that is exposed at the protein surface [49]. A potential cooperation between the PxxP domain and the GPG-motif could explain the impairment on F-actin reorganization and Nef-dependent MHCI-downregulation observed in Nef-PG1/AA or -PG2/AA expressing cells.

The fact that the GPG-motif was dispensable for Nef-induced CD4-downregulation in HeLa-CD4 cells but required in T-cells or HeLa-CD4/p56^{Lck} cells, also suggest that the Nef-GPG-motif would be required for early steps of HIV-1 Nef/p56^{Lck} dislodgement previous to CD4-internalization in T-cells, likely through direct or indirect interaction with p56^{Lck}. A computational prediction using a motif discovery algorithm identified the GPG-loop in HIV-1 Nef as a potential binding site for p56^{Lck}, among other host proteins, in particular its SH2 domain [50]. Since the PxxP motif, the SH3-binding domain in Nef, is intact in Nef-GPG-mutants our ongoing studies are focused to ascertain whether this GPG-motif is involved in the Nef-binding to p56^{Lck}-SH2.

We also observed that the GPG-motif was required for Nef-induced IC recruitment of dually phosphorylated pTyr^{505/394}, potentially into the RE/TGN as previously illustrated in HIV-1 infected T-cells [29]. This hallmark of Nef proteins [30] mostly correlates with its requirement for CD4-downregulation from plasma membrane in p56^{Lck}-expressing cells. Our observations indicate that Nef-dependent IC recruitment of p56^{Lck} already occurs in resting cells, and suggests that HIV-1 Nef could decouple downstream TCR signalling even before TCR-engagement. Since the central GPG-mutants impair Nef’s effects on both IC recruitment of p56^{Lck} and actin-ring formation upon T-cell activation, we expected that Nef-GPG-motif was required for Nef-dependent optimal viral replication and, very likely, for Nef-induced viral spread through cell-to-cell contacts at the virological synapse.

In this line, the breakthrough of this study is the identification of the GPG-motif as a specific molecular element in HIV-1 Nef required for optimal viral infectivity in T-cells. Viruses bearing mutations on the Nef-GPG-motif were as deficient as ΔNef viruses as long as they were produced in T-cells. In contrast, the Nef GPG-motif was dispensable for those viruses

produced in non T-cells. Thus it can also be suggested that p56^{Lck}, among other cellular factors, could be involved in the participation of the GPG-motif in Nef-dependent optimal viral infectivity. Strikingly, p56^{Lck} interacts with and targets HIV-1 Gag to the plasma membrane to connect with Nef and viral components for assembly and release [51,52,53]. Moreover, Nef inhibits the TCR-dependent T-cell activation in HIV-1 infected cells but remotely activates the Ras-Erk pathway by an intracellular pool of catalytically active p56^{Lck} [27]. Therefore, it can be suggested that Nef could recruit p56^{Lck} to ensure the target of viral proteins to membrane platforms for proper assembly and budding through the exocytic machinery in the infected cell.

Finally and in agreement with the presence of conserved short linear motifs (SLIMs) among unrelated viral species [50,54], we have observed that other proteins like Tax (Human T-lymphotropic virus -1 and 2) and EP402R (African swine fever virus) may encode orthologous GPG-motifs as they bear highly homologous protein cassettes (70% to 78% of identity) to the GPG-loop in HIV-1 Nef, (Martinez-Bonet, unpublished results). This recurrence of the Nef-GPG-motif not only suggests an evolutionary mechanism for the acquisition of functional regions by mimicking host machineries but also could allow the design of wide spectrum therapeutic approaches with activity over different infectious viruses.

Supporting Information

S1 Fig. Mutations on the Nef-dimerization motif abrogate Nef-mediated CD4 down-regulation of surface CD4 on T-cells. A-B) CEM cells were transfected with either wild type or the indicated Nef mutants as GFP-fusion proteins and Nef-induced surface CD4 down-regulation was analysed by two-colour flow cytometry in GFP expressing cells. A) The mean fluorescence intensity (MFI) of CD4 (PE) in the GFP-positive cells was used to calculate the individual activity relative to wild-type Nef. Histograms represent the arithmetic mean \pm S.D of at least three independent experiments. ***, $p < 0.001$; n.s. not statistically significant. B) Dot plots and the corresponding MFI are representative of three independent assays. C-D) Peripheral CD3+CD4+ T-cells were transfected with wild type or the indicated Nef mutants as GFP-fusion proteins. C) The mean fluorescence intensity (MFI) of CD4 (PC7) in the GFP-positive cells was used to calculate the Nef activity on surface CD4 expression. Histograms represent the Nef activity of the corresponding GPG mutants relative to wild-type Nef. Values are the arithmetic mean \pm SD of at least three independent experiments. ***, $p < 0.001$. D) The expression of either wild type or the indicated Nef mutants as GFP-fusion proteins was analysed by western blotting. Anti γ -adapatin was used as loading control staining.

S2 Fig. Ectopic expression of p56^{Lck} in HeLa-CD4 cells restores the GPG-requirement for Nef-induced CD4-downregulation. A-B) HeLa-CD4 cells were co-transfected with either the wild type or the indicated Nef-GPG mutants (Nef-GFP) along with an empty (A) or p56^{Lck}-mCherry constructs (B). Nef activity on CD4-downregulation was analysed by indirect immunofluorescent staining. A medial optical section of representative cell is shown. Single Nef-GFP positive cells in (B) are indicated by asterisks, whereas co-transfected cells are indicated by arrows. Areas of co-localization of Nef-GFP and p56^{Lck}-mCherry are seen in yellow. Scale bar, 10 μ m. C-D) The expression of Nef-GFP (C) or Nef-GFP and p56^{Lck}-mCherry (D) was analysed by western blotting. γ -adapatin was used as loading control staining.

S3 Fig. The PPGG-motif is required for Nef-induced intracellular recruitment of p56^{Lck} in peripheral CD4+ T-cells. (A-B) The subcellular distribution of endogenous p56^{Lck} and pTyr⁵⁰⁵-Lck in CD4+ T-cells was analysed by indirect immunofluorescent staining in

peripheral T-cells expressing the wild type or the indicated Nef mutants as GFP fusion proteins. A) A medial optical section of a representative cell is shown. Scale bar, 10 μ m. B) Histograms represent the mean percentage \pm SD of cells with predominant intracellular localization of p56^{Lck}. Values are the arithmetic mean \pm SD of at least three independent experiments in which over 100 cells were counted per condition. ***, $p < 0.001$.

(TIF)

S1 Table. Primers to generate site-specific mutants in HIV-1 Nef NL4.3.

(PDF)

Acknowledgments

We thank the Imaging Facility of IISGM and CBMSO (CSIC/UAM) for technical assistance. The following reagents were obtained through the AIDS research and reference reagent program, Division of AIDS, NIAID, NIH: P4-R5 MAGI from Dr. N. Landau, CEM-SS from Dr. P.L. Nara, Jurkat cells from Dr. A. Weiss and TZM-bl cells from Dr J. C.Kappes, and pNL4.3 Δ nef proviruses was from Dr. J. Gibs. We also thank Dr.S. Benichou (Institut Cochin, France) for kindly providing the pCG-Nef-GFP and pGEX-Nef constructs.

Author Contributions

Conceived and designed the experiments: MM-B OTF RM. Performed the experiments: MM-B CP VB JMR RM. Analyzed the data: MM-B OTF RM. Contributed reagents/materials/analysis tools: MM-B OTF MR MAM-F RM. Wrote the paper: MM-B MR OTF RM.

References

1. Chowder MY, Spina CA, Kwok TJ, Fitch NJ, Richman DD, Guatelli JC (1994) Optimal infectivity in vitro of human immunodeficiency virus type 1 requires an intact nef gene. *J Virol* 68: 2906–2914.
2. Kestier HW, Ringler DJ, Mori K, Panicali DL, Sehgal PK, Daniel MD, et al. (1991) Importance of the nef gene for maintenance of high virus loads and for development of AIDS. *Cell* 65: 651–662. PMID: [2032289](#)
3. Baur AS, Sawai ET, Dazin P, Fantl WJ, Cheng-Mayer C, Peterlin BM (1994) HIV-1 Nef leads to inhibition or activation of T cells depending on its intracellular localization. *Immunity* 1: 373–384. PMID: [7882168](#)
4. Birch MR, Learmont JC, Dyer WB, Deacon NJ, Zaunders JJ, Saksena N, et al. (2001) An examination of signs of disease progression in survivors of the Sydney Blood Bank Cohort (SBBC). *J Clin Virol* 22: 263–270. PMID: [11564591](#)
5. Carl S, Greenough TC, Krumbiegel M, Greenberg M, Skowronski J, Sullivan JL, et al. (2001) Modulation of different human immunodeficiency virus type 1 Nef functions during progression to AIDS. *J Virol* 75: 3657–3665. PMID: [11264355](#)
6. Rodes B, Toro C, Paxinos E, Poveda E, Martinez-Padial M, Benito JM, et al. (2004) Differences in disease progression in a cohort of long-term non-progressors after more than 16 years of HIV-1 infection. *AIDS* 18: 1109–1116. PMID: [15166526](#)
7. Geyer M, Fackler OT, Peterlin BM (2001) Structure—function relationships in HIV-1 Nef. *EMBO J* 20: 580–585.
8. Saksela K (2011) Interactions of the HIV/SIV pathogenicity factor Nef with SH3 domain-containing host cell proteins. *Curr HIV Res* 9: 531–542. PMID: [22103837](#)
9. Laguette N, Bregnard C, Benichou S, Basmaciogullari S (2010) Human immunodeficiency virus (HIV) type-1, HIV-2 and simian immunodeficiency virus Nef proteins. *Mol Aspects Med* 31: 418–433. doi: [10.1016/j.mam.2010.05.003](#) PMID: [20594957](#)
10. Garcia JV, Miller AD (1991) Serine phosphorylation-independent downregulation of cell-surface CD4 by nef. *Nature* 350: 508–511. PMID: [2014052](#)
11. Schwartz O, Marechal V, Le Gall S, Lemonnier F, Heard JM (1996) Endocytosis of major histocompatibility complex class I molecules is induced by the HIV-1 Nef protein. *Nat Med* 2: 338–342. PMID: [8612235](#)
12. Swigut T, Shohdy N, Skowronski J (2001) Mechanism for down-regulation of CD28 by Nef. *EMBO J* 20: 1593–1604. PMID: [11285224](#)

13. Shugars DC, Smith MS, Glueck DH, Nantermet PV, Seillier-Moiseiwitsch F, Swanstrom R (1993) Analysis of human immunodeficiency virus type 1 nef gene sequences present in vivo. *J Virol* 67: 4639–4650. PMID: [8043040](#)
14. Venzke S, Michel N, Allespach I, Fackler OT, Keppler OT (2006) Expression of Nef downregulates CXCR4, the major coreceptor of human immunodeficiency virus, from the surfaces of target cells and thereby enhances resistance to superinfection. *J Virol* 80: 11141–11152. PMID: [16928758](#)
15. Dubey S, Khalid M, Wesley C, Khan SA, Wanchu A, Jameel S (2008) Downregulation of CCR5 on activated CD4 T cells in HIV-infected Indians. *J Clin Virol* 43: 25–31. doi: [10.1016/j.jcv.2008.03.026](#) PMID: [18462992](#)
16. Stumptner-Cuvelette P, Morchoisne S, Dugast M, Le Gall S, Raposo G, Schwartz O, et al. (2001) HIV-1 Nef impairs MHC class II antigen presentation and surface expression. *Proc Natl Acad Sci U S A* 98: 12144–12149. PMID: [11593029](#)
17. Sol-Foulon N, Moris A, Nobile C, Boccaccio C, Engering A, Abastado JP, et al. (2002) HIV-1 Nef-induced upregulation of DC-SIGN in dendritic cells promotes lymphocyte clustering and viral spread. *Immunity* 16: 145–155. PMID: [11825573](#)
18. Craig HM, Pandori MW, Guatelli JC (1998) Interaction of HIV-1 Nef with the cellular dileucine-based sorting pathway is required for CD4 down-regulation and optimal viral infectivity. *Proc Natl Acad Sci U S A* 95: 11229–11234. PMID: [9736718](#)
19. Craig HM, Reddy TR, Riggs NL, Dao PP, Guatelli JC (2000) Interactions of HIV-1 nef with the mu subunits of adaptor protein complexes 1, 2, and 3: role of the dileucine-based sorting motif. *Virology* 271: 9–17. PMID: [10814565](#)
20. Janvier K, Craig H, Hitchin D, Madrid R, Sol-Foulon N, Renault L, et al. (2003) HIV-1 Nef Stabilizes the Association of Adaptor Protein Complexes with Membranes. *J Biol Chem* 278: 8725–8732. PMID: [12486136](#)
21. Rose JJ, Janvier K, Chandrasekhar S, Sekaly RP, Bonifacino JS, Venkatesan S (2005) CD4 Down-regulation by HIV-1 and Simian Immunodeficiency Virus (SIV) Nef Proteins Involves Both Internalization and Intracellular Retention Mechanisms. *J Biol Chem* 280: 7413–7426. PMID: [15611114](#)
22. Madrid R, Janvier K, Hitchin D, Day J, Coleman S, Noviello C, et al. (2005) Nef-induced Alteration of the Early/Recycling Endosomal Compartment Correlates with Enhancement of HIV-1 Infectivity. *J Biol Chem* 280: 5032–5044. PMID: [15569681](#)
23. Coleman SH, Madrid R, Van Damme N, Mitchell RS, Bouchet J, Servant C, et al. (2006) Modulation of Cellular Protein Trafficking by Human Immunodeficiency Virus Type 1 Nef: Role of the Acidic Residue in the ExxxLL Motif. *J Virol* 80: 1837–1849. PMID: [16439540](#)
24. Laguette N, Bregnard C, Bouchet J, Benmerah A, Benichou S, Basmaciogullari S (2009) Nef-Induced CD4 Endocytosis in Human Immunodeficiency Virus Type 1 Host Cells: Role of p56lck Kinase. *J Virol* 83: 7117–7128. doi: [10.1128/JVI.01648-08](#) PMID: [19439470](#)
25. Collette Y, Dutartre H, Benziane A, Ramos M, Benarous R, Harris M, et al. (1996) Physical and functional interaction of Nef with Lck. HIV-1 Nef-induced T-cell signaling defects. *J Biol Chem* 271: 6333–6341. PMID: [8626429](#)
26. Burtey A, Rappoport JZ, Bouchet J, Basmaciogullari S, Guatelli J, Simon SM, et al. (2007) Dynamic Interaction of HIV-1 Nef with the Clathrin-Mediated Endocytic Pathway at the Plasma Membrane. *Traffic* 8: 61–76. PMID: [17140399](#)
27. Thoulouze MI, Sol-Foulon N, Blanchet F, Dautry-Varsat A, Schwartz O, Alcover A (2006) Human immunodeficiency virus type-1 infection impairs the formation of the immunological synapse. *Immunity* 24: 547–561. PMID: [16713973](#)
28. Haller C, Rauch S, Fackler OT (2007) HIV-1 Nef Employs Two Distinct Mechanisms to Modulate Lck Subcellular Localization and TCR Induced Actin Remodeling. *PLoS ONE* 2: e1212. PMID: [18030346](#)
29. Pan X, Rudolph JM, Abraham L, Habermann A, Haller C, Krijnse-Locker J, et al. (2012) HIV-1 Nef compensates for disorganization of the immunological synapse by inducing trans-Golgi network-associated Lck signaling. *Blood* 119: 786–797. doi: [10.1182/blood-2011-08-373209](#) PMID: [22123847](#)
30. Rudolph JM, Eickel N, Haller C, Schindler M, Fackler OT (2009) Inhibition of T cell receptor induced actin remodeling and relocation of Lck are evolutionarily conserved activities of lentiviral Nef proteins. *J Virol* 82: 11528–11539.
31. Saksela K, Cheng G, Baltimore D (1995) Proline-rich (PxxP) motifs in HIV-1 Nef bind to SH3 domains of a subset of Src kinases and are required for the enhanced growth of Nef+ viruses but not for down-regulation of CD4. *EMBO J* 14: 484–491. PMID: [7859737](#)
32. Greenberg ME, Lafrate AJ, Skowronski J (1998) The SH3 domain-binding surface and an acidic motif in HIV-1 Nef regulate trafficking of class I MHC complexes. *EMBO J* 17: 2777–2789. PMID: [9582271](#)

33. Fackler OT, Luo W, Geyer M, Alberts AS, Peterlin BM (1999) Activation of Vav by Nef induces cytoskeletal rearrangements and downstream effector functions. pp. 729–739.
34. Stolp B, Abraham L, Rudolph JM, Fackler OT (2010) Lentiviral Nef proteins utilize PAK2-mediated deregulation of cofilin as a general strategy to interfere with actin remodeling. *J Virol* 84: 3935–3948. doi: [10.1128/JVI.02467-09](https://doi.org/10.1128/JVI.02467-09) PMID: [20147394](https://pubmed.ncbi.nlm.nih.gov/20147394/)
35. Bunnell SC, Kapoor V, Tribble RP, Zhang W, Samelson LE (2001) Dynamic actin polymerization drives T cell receptor-induced spreading: a role for the signal transduction adaptor LAT. *Immunity* 14: 315–329. PMID: [11290340](https://pubmed.ncbi.nlm.nih.gov/11290340/)
36. Guyader M, Kiyokawa E, Abrami L, Turelli P, Trono D (2002) Role for Human Immunodeficiency Virus Type 1 Membrane Cholesterol in Viral Internalization. *J Virol* 76: 10356–10364. PMID: [12239312](https://pubmed.ncbi.nlm.nih.gov/12239312/)
37. Nika K, Soldani C, Salek M, Paster W, Gray A, Etzensperger R, et al. Constitutively active Lck kinase in T cells drives antigen receptor signal transduction. *Immunity* 32: 766–777. doi: [10.1016/j.immuni.2010.05.011](https://doi.org/10.1016/j.immuni.2010.05.011) PMID: [20541955](https://pubmed.ncbi.nlm.nih.gov/20541955/)
38. Haller C, Rauch S, Michel N, Hannemann S, Lehmann MJ, Keppler OT, et al. (2006) The HIV-1 pathogenicity factor Nef interferes with maturation of stimulatory T-lymphocyte contacts by modulation of N-Wasp activity. *J Biol Chem* 281: 19618–19630. PMID: [16687395](https://pubmed.ncbi.nlm.nih.gov/16687395/)
39. Stolp B, Reichman-Fried M, Abraham L, Pan X, Giese SI, Hannemann S, et al. (2009) HIV-1 Nef Interferes with Host Cell Motility by Deregulation of Cofilin. *Cell Host & Microbe* 6: 174–186.
40. Stolp B, Imle A, Coelho FM, Hons M, Gorina R, Lyck R, et al. (2012) HIV-1 Nef interferes with T-lymphocyte circulation through confined environments in vivo. *Proc Natl Acad Sci U S A* 109: 18541–18546. doi: [10.1073/pnas.1204322109](https://doi.org/10.1073/pnas.1204322109) PMID: [23093676](https://pubmed.ncbi.nlm.nih.gov/23093676/)
41. Abraham L, Bankhead P, Pan X, Engel U, Fackler OT (2012) HIV-1 Nef Limits Communication between Linker of Activated T Cells and SLP-76 To Reduce Formation of SLP-76-Signaling Microclusters following TCR Stimulation. *J Immunol* 189: 1898–1910. doi: [10.4049/jimmunol.1200652](https://doi.org/10.4049/jimmunol.1200652) PMID: [22802418](https://pubmed.ncbi.nlm.nih.gov/22802418/)
42. Imle A, Abraham L, Tsopoulidis N, Hoflack B, Saksela K, Fackler OT (2015) Association with PAK2 Enables Functional Interactions of Lentiviral Nef Proteins with the Exocyst Complex. *mBio* 6.
43. Manninen A, Huotari Pi, Hiipakka M, Renkema GH, Saksela K (2001) Activation of NFAT-Dependent Gene Expression by Nef: Conservation among Divergent Nef Alleles, Dependence on SH3 Binding and Membrane Association, and Cooperation with Protein Kinase C. *J Virol* 75: 3034–3037. PMID: [11222731](https://pubmed.ncbi.nlm.nih.gov/11222731/)
44. Agopian K, Wei BL, Garcia JV, Gabuzda D (2006) A Hydrophobic Binding Surface on the Human Immunodeficiency Virus Type 1 Nef Core Is Critical for Association with p21-Activated Kinase 2. *J Virol* 80: 3050–3061. PMID: [16501114](https://pubmed.ncbi.nlm.nih.gov/16501114/)
45. Meuwissen P, Stolp B, Iannucci V, Vermeire J, Naessens E, Saksela K, et al. (2012) Identification of a highly conserved valine-glycine-phenylalanine amino acid triplet required for HIV-1 Nef function. *Retrovirology* 9: 34. doi: [10.1186/1742-4690-9-34](https://doi.org/10.1186/1742-4690-9-34) PMID: [22537596](https://pubmed.ncbi.nlm.nih.gov/22537596/)
46. Haller C, Tibroni N, Rudolph JM, Grosse R, Fackler OT (2011) Nef does not inhibit F-actin remodelling and HIV-1 cell-cell transmission at the T lymphocyte virological synapse. *Eur J Cell Biol* 90: 913–921. doi: [10.1016/j.ejcb.2010.09.010](https://doi.org/10.1016/j.ejcb.2010.09.010) PMID: [21044805](https://pubmed.ncbi.nlm.nih.gov/21044805/)
47. Roeth JF, Williams M, Kasper MR, Filzen TM, Collins KL (2004) HIV-1 Nef disrupts MHC-I trafficking by recruiting AP-1 to the MHC-I cytoplasmic tail. *J Cell Biol* 167: 903–913. PMID: [15569716](https://pubmed.ncbi.nlm.nih.gov/15569716/)
48. Atkins KM, Thomas L, Youker RT, Harriff MJ, Pissani F, You H, et al. (2008) HIV-1 Nef Binds PACS-2 to Assemble a Multikinase Cascade That Triggers Major Histocompatibility Complex Class I (MHC-I) Down-regulation: Analysis Using Short Interfering RNA and Knock-out Mice. *J Biol Chem* 283: 11772–11784. doi: [10.1074/jbc.M707572200](https://doi.org/10.1074/jbc.M707572200) PMID: [18296443](https://pubmed.ncbi.nlm.nih.gov/18296443/)
49. Grzesiek S, Bax A, Hu JS, Kaufman J, Palmer I, Stahl SJ, et al. (1997) Refined solution structure and backbone dynamics of HIV-1 Nef. *Prot Sci* 6: 1248–1263.
50. Sarmady M, Dampier W, Tozeren A (2011) Sequence- and Interactome-Based Prediction of Viral Protein Hotspots Targeting Host Proteins: A Case Study for HIV Nef. *PLoS ONE* 6: e20735. doi: [10.1371/journal.pone.0020735](https://doi.org/10.1371/journal.pone.0020735) PMID: [21738584](https://pubmed.ncbi.nlm.nih.gov/21738584/)
51. Strasner AB, Natarajan M, Doman T, Key D, August A, Henderson AJ (2008) The Src Kinase Lck Facilitates Assembly of HIV-1 at the Plasma Membrane. *J Immunol* 181: 3706–3713. PMID: [18714047](https://pubmed.ncbi.nlm.nih.gov/18714047/)
52. von Schwedler UK, Stuchell M, Muller B, Ward DM, Chung HY, Morita E, et al. (2003) The protein network of HIV budding. *Cell* 114: 701–713. PMID: [14505570](https://pubmed.ncbi.nlm.nih.gov/14505570/)
53. Costa L, Chen N, Lopes A, Aguiar R, Tanuri A, Plemenitas A, et al. (2006) Interactions between Nef and AIP1 proliferate multivesicular bodies and facilitate egress of HIV-1. *Retrovirology* 3: 33. PMID: [16764724](https://pubmed.ncbi.nlm.nih.gov/16764724/)
54. Davey NE, Trave G, Gibson TJ (2011) How viruses hijack cell regulation. *Trends Biochem Sci* 36: 159–169. doi: [10.1016/j.tibs.2010.10.002](https://doi.org/10.1016/j.tibs.2010.10.002) PMID: [21146412](https://pubmed.ncbi.nlm.nih.gov/21146412/)